Carbohydrate Polymers 79 (2010) 981–988

Contents lists available at ScienceDirect

Carbohydrate Polymers

journal homepage: www.elsevier.com/locate/carbpol

Effect of temperature on the dynamic and steady-shear rheology of a new microbial extracellular polysaccharide produced from glycerol byproduct

Vítor D. Alves [a,*], Filomena Freitas [b], Nuno Costa [b], Mónica Carvalheira [b], Rui Oliveira [b], Maria P. Gonçalves [a], Maria A.M. Reis [b]

[a] REQUIMTE-Department of Chemical Engineering, Faculty of Engineering, Universidade do Porto, Rua Dr. Roberto Frias s/n, 4200-465 Porto, Portugal
[b] REQUIMTE/CQFB, Chemistry Department, FCT/Universidade Nova de Lisboa, 2829-516 Caparica, Portugal

ARTICLE INFO

Article history:
Received 8 July 2009
Received in revised form 22 September 2009
Accepted 13 October 2009
Available online 17 October 2009

Keywords:
Rheology
Temperature
Extracellular polysaccharide
Glycerol-rich product
Pseudomonas oleovorans

ABSTRACT

The effect of temperature on the dynamic and steady-shear rheology of aqueous solutions of an extracellular polysaccharide produced by microbial fermentation using *Pseudomonas oleovorans* NRRL B-14682 and glycerol byproduct, was studied. The biopolymer solutions have shown a pseudoplastic fluid behaviour and no gel formation was detected for all temperatures studied. As expected, the steady shear and dynamic parameters decreased with increasing temperature, due to the increase of polymer chain mobility. The EPS solutions were thermorheologically simple and stable, since the rheological parameters were successfully superimposed to and arbitrary reference temperature using the Time–Temperature Superposition principle, and the Cox-Merz rule was satisfactorily applied. In addition, the rheological properties were maintained under consecutive oscillatory and steady-state tests at 25 °C, after exposing the sample to increasing temperatures up to 80 °C. This polymer is a good candidate to be used in industrial processes involving temperature variations, at least in the range from 15 to 80 °C.

1. Introduction

Polysaccharides from natural sources are a class of compounds that are broadly used in many areas of application, such as in the food, pharmaceutical and cosmetic industries (as thickeners, gelling agents, texture modifiers, stabilizers and binding agents), in the paper industry (as strengthening agents), in oil well fracturing and drilling, in water treatment and mining industry (as flocculating agents), and in biodegradable films for agricultural purposes and packaging.

Natural biopolymers have been recovered from plants, e.g. galactomannans, starch, and pectins (Cerqueira et al., 2009; Nwokocha & Williams, 2009a; Wang et al., 2007); from algae, e.g. carrageenan, alginate and agar (Gomez, Lambrecht, Lozano, Rinaudo, & Villar, 2009; Hilliou et al., 2006; Villanueva, Sousa, Gonçalves, Nilsson, & Hilliou, 2009); and animal sources, e.g. chitosan (Abdou, Nagy, & Elsabee, 2008). However, the characteristics and availability of the recovered products are dependent on the season of the year and climate conditions. As an alternative, polysaccharides may well be obtained by microbial fermentation, e.g. xanthan gum, bacterial alginate, levan and succinoglycan (Bae, Oh, Lee, Yoo, & Lee, 2008; García-Ochoa, Santos, Casas, & Gómez, 2000; Peña, Trujillo-Roldán, & Galindo, 2000; Simsek, Mert, Campanella, & Reuhs, 2009), since they are naturally produced by several microorganisms. Microbial fermentation is a more controlled process depending only on manipulated variables that, under optimized conditions, enables the production of key compounds at a constant rate and with unchanged properties over time. Besides the polysaccharide physicochemical characterization, the evaluation of the influence of different parameters, such as temperature and polymer concentration, on the rheological properties of their aqueous solutions, is essential (Arvidson, Rinehart, & Gadala-Maria, 2006; Bae et al., 2008; Nickerson, Paulson, & Speers, 2004; Simsek et al., 2009; Xu, Liu, & Zhang, 2006).

The production of a new extracellular polysaccharide (EPS) by microbial fermentation with a *Pseudomonas oleovorans* strain has been previously reported, using pure glycerol (Freitas et al., 2009a) and glycerol byproduct from the biodiesel manufacture without any pre-treatment (Freitas et al., 2009b). The EPS produced in both cases is a high molecular weight heteropolysaccharide ($1.0–5.0 \times 10^6$) with good viscous enhancing properties, and composed by neutral sugars and acyl groups, the later conferring a small charge density to the polymer chains. From the study of the properties in aqueous solutions of the EPS produced from pure glycerol, the zero-shear rate scaling with concentration in salt free solutions revealed to follow a typical polyelectrolyte behaviour in a bad solvent, while at high ionic strength the rheological properties

* Corresponding author. Present address: CEER – Biosystems Engineering, Instituto Superior de Agronomia – UTL, Tapada da Ajuda, 1349-017 Lisboa, Portugal. Tel.: +351 213653546; fax: +351 213653200.
E-mail address: vitoralves@isa.utl.pt (V.D. Alves).

0144-8617/$ - see front matter © 2009 Elsevier Ltd. All rights reserved.
doi:10.1016/j.carbpol.2009.10.026

are similar to that of neutral polymers. In addition, the EPS has shown to adopt a globular conformation as a result of hydrophobic interactions (Hilliou et al., 2009).

EPS production using glycerol byproduct without any purification step is of major interest, since it constitutes a low cost carbon source, contributing to the reduction of the overall production costs. Even though the polymer characteristics in terms of composition and average molecular weight were not significantly influenced by the use of the glycerol byproduct instead of pure glycerol, the EPS must be further characterized in order to infer about its potential applications. Preliminary studies on the effect of polymer concentration, pH, ionic strength and temperature on the apparent viscosity of aqueous solutions of the EPS produced from glycerol byproduct, were already presented in a previous work (Freitas et al., 2009b). However, a deeper insight on the biopolymer rheological properties is required, for example to evaluate how they are affected by temperature. Temperature variations are encountered in many industrial processes, namely in the food industry (e.g. in sterilization, evaporation, drying and extrusion operations), and it is of major importance the evaluation of the viscoelastic properties of EPS solutions in such conditions.

In this work, a detailed study concerning the effect of temperature on the dynamic and steady-shear rheology of EPS solutions, in the temperature range between 15 and 80 °C, was performed.

2. Materials and methods

2.1. Biopolymer production, extraction and characterization

The biopolymer was produced by *P. oleovorans* NRRL B-14682 grown on a slightly modified Medium E* (Freitas et al., 2009a), supplemented with glycerol-rich product. The cultivation was performed in a 10 L bioreactor (BioStat B-plus, Sartorius), as described by Freitas et al. (2009a). Culture broth samples were recovered from the bioreactor along the cultivation run and centrifuged (18,000*g*, 15 min) for cell separation. The cell-free supernatant was stored at −20 °C for the determination of glycerol and ammonium concentrations. Cell dry weight, glycerol and ammonium concentrations were determined as described by Freitas et al. (2009a).

The biopolymer was extracted from the culture broth as described by Freitas et al. (2009b). Briefly, the culture broth was diluted with deionised water for viscosity reduction and centrifuged (20,000*g* for 1 h) for cell separation. The biopolymer in the cell-free supernatant was precipitated by the addition of cold acetone (3:1), dissolved in deionised water and freeze dried. The biopolymer thus obtained, referred to as semi-purified EPS, was further purified by performing the acetone precipitation procedure twice followed by dialysis with a 3500 MWCO membrane (SnakeSkinTM Pleated Dialysis Tubing 68035 – Thermo Scientific), against deionised water, for 48 h. The dialysis solution contained 6 ppm sodium azide (Sigma–Aldrich) to avoid biological degradation of the samples. After dialysis the polymer solution was freeze dried.

The extracted EPS was characterized in terms of its sugar composition, acyl groups, inorganic and protein content as described by Freitas et al., 2009b. Average molecular weights and the polydispersity indexes were obtained by size exclusion chromatography, as described by Freitas et al. (2009a).

2.2. Preparation of solutions

The purified freeze dried polymer was gradually added to a specific volume of distilled water in order to obtain a polymer concentration of 0.85 wt%, which was constant in all the experiments. Sodium azide (Sigma–Aldrich) was added to prevent microbial growth, at a concentration of 10 ppm. The solution was vigorously stirred at room temperature during 16 h, and was degassed in a vacuum chamber before the experiments.

From the study of the concentration regimes, the transition from the semi-dilute to the concentrated regime takes place at $C^{**} \approx 0.42$ wt% (unpublished data), thus the 0.85 wt% polymer solution used throughout this work is in the concentrated regime.

2.3. Rheological measurements

The rheological measurements were carried out using a controlled stress rheometer (AR2000, TA Instruments) with a cone and plate geometry (cone angle of 2° and a diameter of 40 mm). The solution flow curves were obtained performing steady stress sweep tests (shear rate measured over the last 20 s of a step shear stress during 60 s, and steady-state defined within a 5% tolerance for shear rate variation between two consecutive step shear stresses), in the shear rate range between 0.1 and 700 s^{-1}. The mechanical spectra of the samples were recorded before and after the steady-state measurements, by performing a frequency sweep (0.1–100 rad/s) obtained with an oscillatory strain amplitude of 0.2. The strain amplitude was chosen based on strain sweeps at constant frequency, in order to assure conditions within the linear viscoelastic region. Both oscillatory and steady-state tests were carried out in the temperature range from 15 to 65 °C. The samples were covered with a thin layer of paraffin oil to prevent water evaporation. No emulsion between the samples and the paraffin oil was detected within the range of applied stresses.

Some of the measurements were carried out in triplicate. The reproducibility of the results was quite good, since the deviation from the mean value was below 5% for the apparent viscosity and G'', and below 10% for G'.

2.4. Calculations

The non-linear fitting calculations were carried out using the software package Scientis™, from MicroMath®. The errors associated with the determined parameters were calculated within a confidence interval of 95%.

3. Results and discussion

3.1. Biopolymer production and physicochemical characterization

The biopolymer produced by *P. oleovorans* from glycerol byproduct was recovered from the culture broth after 5 days of cultivation in a fed-batch reactor. The final EPS concentration in the broth was 15.0 g L^{-1}, corresponding to a productivity of 0.13 g L^{-1} h^{-1} and a net yield of EPS on glycerol of 0.15 g g^{-1}. A more detailed description of the production process is presented in a previous work, Freitas et al., 2009b.

The glycosyl composition analysis of the purified EPS revealed that it was mainly composed by galactose that represented 68% of the polymer's carbohydrate content. The other sugar components were mannose (17%), glucose (13%), fucose (4%) and rhamnose (2%). The polymer also had acyl groups substituents that accounted for 3.93% of its dry mass. The main acyl groups detected were pyruvil (3.24%) and succinyl (0.70%). Other non-sugar components, namely, proteins and ashes, accounted for 6.54% and 1.10%, respectively, of the purified EPS dry mass (Freitas et al., 2009b). The EPS had an average molecular weight of 4.6×10^6, being rather homogeneous, as shown by the polidispersity index of 2.31.

The intrinsic viscosity of the purified polymer was determined by double extrapolation of the Huggins and Kraemer equations, respectively:

$$\frac{\eta_{sp}}{C} = [\eta] + k_H[\eta]^2 C \quad (1)$$

$$\frac{\ln(\eta_{rel})}{C} = [\eta] + k_k[\eta]^2 C \quad (2)$$

where $[\eta]$, η_{sp} and η_{rel} are the intrinsic, specific and relative viscosities, respectively; k_H and k_k are the Huggins and Kraemer coefficients, and C is the polymer concentration. The viscosity of dilute solutions was measured using a Cannon Fenske capillary viscometer. The solutions had relative viscosities in the range between 1.2 and 2.0, in order to ensure a good accuracy and linearity in the extrapolations to zero concentration. The value obtained for $[\eta]$ was 10.9 dL/g, which is much higher than that reported for the EPS produced from pure glycerol (6.2 dL/g) (Hilliou et al., 2009), at the same ionic strength (NaCl 0.1 M). The higher intrinsic viscosity is in agreement with the lower Huggins coefficient obtained, $k_H = 0.6$ ($k_H = 2.6$ for the EPS produced from pure glycerol). Values of k_H are, in theory, independent of molecular masses but depend on solute–solvent interactions and on the state of aggregation of macromolecules. The value of $k_H = 0.6$ may reflect some intermolecular aggregation as for flexible macromolecules in a good solvent, $k_H \approx 0.3$. The value of $k_H = 2.6$ for the EPS produced from pure glycerol is indicative of high intermolecular aggregation, however, light scattering data for this polymer indicated a non-significant aggregation in the samples stored up to 4 days. Thus, additional light scattering experiments are needed to check the polymer chain conformation (Hilliou et al., 2009).

These results suggest that the two polymers behave differently in solution, with the EPS from glycerol byproduct presenting less intra or intermolecular interactions, which may be caused by the acyl groups in the polymer backbone (Rinaudo, 2004). This may lead to a more extended conformation originating a higher intrinsic viscosity. However, further studies are needed to fully characterize the solution properties of both polymers.

3.2. Rheological properties

3.2.1. Rheological behaviour under continuous shear flow

The flow curves obtained for the 0.85 wt% purified exopolysaccharide solution, at the different temperatures studied, are presented in Fig. 1A. The apparent viscosity was measured increasing the shear rate, from nearly 1 s^{-1} up to 700 s^{-1}, immediately followed by a shear rate reduction back to 1 s^{-1}. No hysteresis phenomena were detected for all temperatures tested, as the flow curves obtained were coincident. These results are in agreement to that presented previously for a less purified sample of the same polymer studied in this work (Freitas et al., 2009b).

The apparent viscosity decreased as the temperature increased but the pseudoplastic behaviour was maintained. An approach to a Newtonian plateau at lower shear rates is observed, which is more evident as the temperature was increased, followed by shear-thinning at higher shear rate values. The high molecular weight polymer molecules establish interactions in solution, such as entanglements and hydrogen, electrostatic and hydrophobic bonds. When low shear rates are applied, the rate of disruption of these interactions is similar to that of creation of new ones, resulting in a constant apparent viscosity (Newtonian plateau). At high shear rates, the disruption rate of the interactions predominates and the molecules align in the direction of the flow, resulting in the decrease of the apparent viscosity with the increase of the shear rate (shear-thinning). We observe that the transition from the Newtonian regime to the shear-thining regime moves to higher shear rates as the temperature increases (Fig. 1A), which means that the formation of new interactions is faster at higher temperatures.

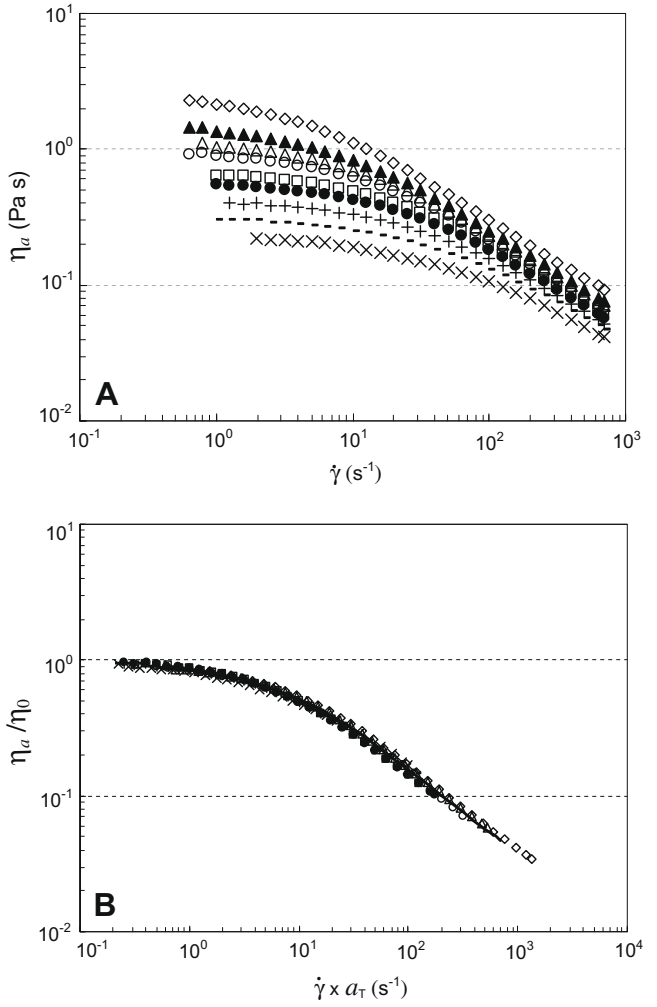

Fig. 1. Flow curves (A) and master curve from Time–Temperature Superposition (B), for a 0.85%wt EPS solution at different temperatures: (◇) 15 °C, (▲) 25 °C, (△) 30 °C, (○) 35 °C, (□) 40 °C, (●) 45 °C, (+) 50 °C; (−) 55 °C, (×) 65 °C.

The Cross (Eq. (3)) and Carreau (Eq. (4)) flow models (Cross, 1965; Carreau, 1972) were used to describe the flow behaviour at different temperatures:

$$\eta_a = \frac{\eta_0}{1 + (\tau\dot{\gamma})^m} \quad (3)$$

$$\eta_a = \frac{\eta_0}{[1 + (\lambda\dot{\gamma})^2]^N} \quad (4)$$

in which the viscosity of the second Newtonian plateau (at infinite shear rate) was neglected, that is valid in this work since it was never approached. $\dot{\gamma}$ represents the shear rate (s^{-1}), η_a is the apparent viscosity (Pa.s), η_0 is the zero-shear rate viscosity (Pa.s), τ and λ are time constants (s), and m and N are dimensionless constants which may be related to the exponent of the power law (n) by $m = 1 - n$ and $N = (1 - n)/2$. These models were chosen in order to estimate both zero-shear rate viscosity and relaxation time constants. The values and errors of the parameters obtained by fitting Eqs. (3) and (4) to the experimental data are presented in Table 1.

Even though both models fitted quite well the experimental results, there was a slight deviation of the Carreau model from experimental data for shear rates approaching 700 s^{-1}, which did not occur with the Cross model (fittings not shown). Nevertheless, in general, both models predicted a decrease of η_0, m and N values with the increase of temperature, which was expected due to the

Table 1
Parameters of the Cross and Carreau models for the range of temperatures studied.

C (wt%)	T (°C)	η_o (Pa s)	τ (s)	m	SSD (10^{-3})
Cross model					
0.85	15	2.677 ± 0.036	0.156 ± 0.007	0.750 ± 0.013	
	25	1.611 ± 0.022	0.094 ± 0.005	0.745 ± 0.015	
	30	1.145 ± 0.021	0.055 ± 0.004	0.791 ± 0.030	
	35	0.995 ± 0.014	0.053 ± 0.003	0.753 ± 0.019	
	40	0.689 ± 0.007	0.032 ± 0.001	0.792 ± 0.017	
	45	0.583 ± 0.004	0.028 ± 0.001	0.773 ± 0.010	
	50	0.428 ± 0.003	0.020 ± 0.001	0.766 ± 0.012	
	55	0.325 ± 0.003	0.018 ± 0.001	0.707 ± 0.013	
	65	0.245 ± 0.003	0.015 ± 0.001	0.661 ± 0.020	
C		(wt%)	T (°C)	η_o (Pa s)	λ
N	SSD	(10^{-3})			
Carreau model					
0.85	15	2.218 ± 0.053	0.395 ± 0.053	0.260 ± 0.015	54.6
	25	1.384 ± 0.034	0.285 ± 0.045	0.246 ± 0.017	33.4
	30	1.037 ± 0.020	0.200 ± 0.030	0.245 ± 0.018	19.7
	35	0.884 ± 0.020	0.191 ± 0.034	0.236 ± 0.019	17.5
	40	0.622 ± 0.011	0.116 ± 0.016	0.242 ± 0.017	4.9
	45	0.527 ± 0.011	0.108 ± 0.017	0.232 ± 0.018	4.4
	50	0.387 ± 0.010	0.084 ± 0.014	0.224 ± 0.017	2.2
	55	0.292 ± 0.010	0.088 ± 0.017	0.199 ± 0.017	1.5
	65	0.217 ± 0.010	0.087 ± 0.018	0.179 ± 0.015	0.8

decrease of the shear-thining behaviour. In addition, the relaxation times also decreased with increasing temperature, meaning that the rate of formation of new interactions between molecules increases over the rate of their disruption, which is in agreement with the shift to higher shear rates of the transition from the Newtonian to the shear-thining regime.

The flow curves could be superimposed to a reference temperature of 25 °C, by scaling vertically with the respective zero-shear viscosity and horizontally with a shift factor (a_T). The superimposed curves are presented in Fig. 1B. The horizontal shift factor increases as the applied temperature decreases (Table 2), which is in agreement with the degree of interactions. Even though the relaxation times are higher at lower temperatures (Table 1), meaning that more time is needed to create new interactions, the overall interaction degree is higher, explaining the higher apparent viscosity.

3.2.2. Viscoelastic behaviour under oscillatory shear flow

Frequency sweeps were performed before and after the steady-state measurements and the obtained spectra were coincident for all temperatures tested (results not shown). This means that the EPS solutions did not change their viscoelastic properties, even after being subjected to shear rates as high as 700 s^{-1}. These properties, along with the ability of the polymer solutions to recover their viscosity after being subjected to high shear rates, makes the polymer a good candidate to be used in industrial applications, namely in the food industry, involving exposure to high shear stresses and temperature variations, simultaneously.

In Fig. 2A, the frequency sweeps for the temperatures of 15 and 65 °C are presented. A characteristic behaviour of macromolecular solutions, in which no gelation process occurs, can be observed. The same behaviour was observed in previous studies with aqueous solutions of samples of the galactose-rich polysaccharide produced by the same bacteria, but using pure glycerol as the sole carbon source (Freitas et al., 2009a; Hilliou et al., 2009). At low frequencies, the loss modulus (G'') is higher than the storage modulus (G'), which means the polymer solution behaves essentially as a liquid. However, at high frequencies a cross-over is detected at 15 °C, after which the elastic contribution predominates, but the same does not happen at 65 °C. These two behaviours were noticed for the other temperatures tested, and may be perceived analyzing Fig. 2B, where Tan (δ) (= G''/G') is presented as a function of the applied frequency. For temperatures above 45 °C, Tan (δ) is higher than 1.0 in all the frequencies range studied, which means that G'' is always higher than G' and no crossover occurs. On the other hand, for $T \leqslant 40$ °C a crossover is detected, and it happens gradually at lower frequency values as the temperature decreases. The lower the temperature, the higher the viscosity and less energy is needed to transfer to the sample in order to store more energy than that dissipated.

Table 2
Shift factors used to apply the Time–Temperature Superposition principle to the dynamic moduli and flow data (T_0 = 25 °C).

	G'		G''		η_a
T (°C)	a_T	b_T	a_T	b_T	a_T
15	2.0	1.1	2.0	1.1	2.0
25	1.0	1.0	1.0	1.0	1.0
30	0.74	0.93	0.75	0.92	0.80
35	0.45	0.74	0.46	0.74	0.51
40	0.30	0.70	0.30	0.70	0.32
45	0.21	0.50	0.19	0.60	0.23
50	0.15	0.50	0.14	0.54	0.20
55	0.095	0.48	0.075	0.47	0.15
65	0.070	0.45	0.050	0.39	0.10

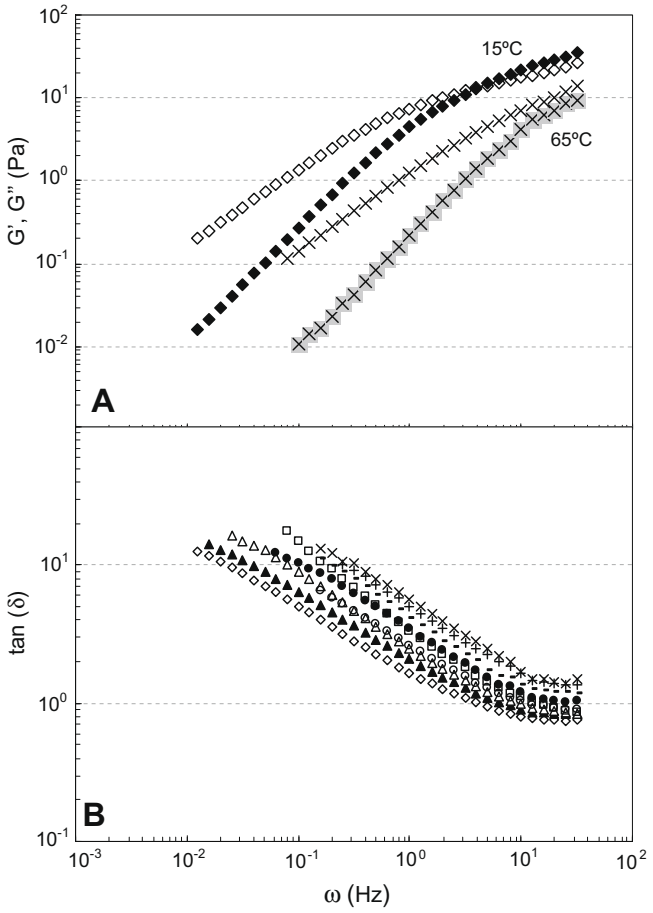

Fig. 2. (A) Mechanical spectra of a 0.85%wt EPS solution at 15 and 65 °C (G'': open symbols, G': full symbols). (B) Tangent of the loss angle, Tan (δ), as a function of the applied frequency for the temperatures studied: (◇) 15 °C, (▲) 25 °C, (△) 30 °C, (○) 35 °C, (□) 40 °C, (●) 45 °C, (+) 50 °C; (−) 55 °C, (×) 65 °C.

The oscillatory isothermal frequency data of viscoelastic variables determined in the temperature range studied, were superimposed to form a single master curve using the Time–Temperature Superposition principle (TTS) (Ferry, 1980). This principle suggests that all contributions to the dynamic moduli should be proportional to $T\rho$, and it is based on the assumption that all relaxation times have the same temperature dependence. In this way, a change of temperature from T to a reference temperature T_0, would cause a change of the moduli G' and G'' equivalent to their multiplication by the temperature density ratio $(T_0\rho_0/T\rho)$, and by shifting horizontally using the temperature dependent shift factor a_T (Da Silva, Gonçalves, & Rao, 1994; Roth, Vega, Vallés, & Villar, 2004). Even though a_T is a parameter determined empirically, it represents the ratio of maximum relaxation times at different temperatures to the maximum relaxation time at the reference temperature (Vinogradov & Malkin, 1980). In this work, there was the need of vertical shifts slightly higher than those obtained from the temperature density ratio. Thus, the adjacent isothermal frequency curves were shifted vertically using the parameter $b_T = b'_T(T_0\rho_0/T\rho)$, where T_0 is the arbitrary selected reference temperature (T_0 = 25 °C).

The frequency/temperature superposition of both moduli is presented in Fig. 3 and the shift factors for each temperature are shown in Table 2. It can be seen that both master curves were obtained with pretty similar shift values, which suggest that the solution is thermorheologically simple, with relaxation times for all mechanisms changing in the same manner with temperature (Nickerson et al., 2004). The same behaviour was presented for galactomannans, such as locust bean gum (da Silva et al., 1994). However, a significant difference of a_T values between the master curves of G' and G'' was encountered for the temperatures of 55 and 65 °C; and also between the a_T values from the flow master curve for 50, 55 and 65 °C and that obtained for G' and G'' for those temperatures. The work of da Silva et al. (1994) with pectin dispersions revealed an unsuccessful application of Time–Temperature Superposition principle in all range of temperatures studied (from 5 to 65 °C). It was attributed to aggregation phenomena as a consequence of important intermolecular interactions, like hydrogen bonds and hydrophobic interactions, and to structural changes of those aggregates with the variation of temperature. Thus, the relaxation processes may be due to different mechanisms and have a different dependence on temperature. A similar behaviour may be occurring with the EPS solution, exhibiting a slightly different dependence on temperature of the different interactions that can occur between polymer molecules (entanglements, hydrogen, electrostatic and hydrophobic bonds), for temperature values above 50 °C.

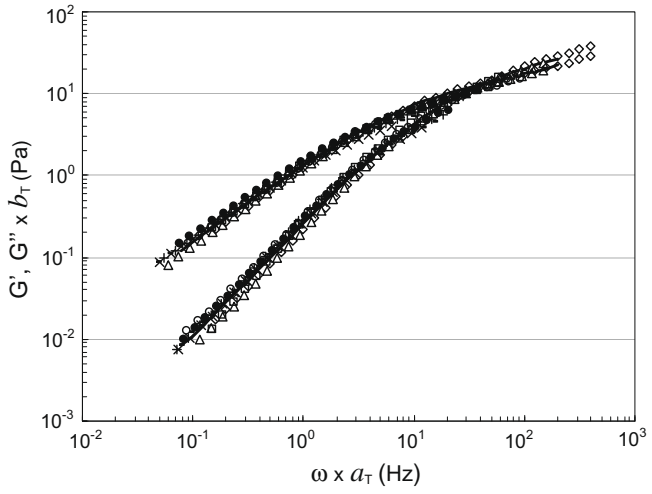

Fig. 3. Frequency/temperature superposition of the loss (G'') and storage (G') moduli. The solid line represents the data for the reference temperature (25 °C) and the symbols correspond to the other temperatures: (◇) 15 °C, (▲) 30 °C, (○) 35 °C, (□) 40 °C, (●) 45 °C, (+) 50 °C; (−) 55 °C, (×) 65 °C.

3.2.3. Effect of temperature on the viscoelastic parameters

The temperature dependence of the apparent viscosity is usually described by the Arrhenius equation:

$$\eta_a = A \exp\left(\frac{E_a}{RT}\right) \quad (5)$$

where A is the pre-exponential factor, E_a is the activation energy, R is the gas constant and T is the absolute temperature. The effect of temperature on the zero-shear rate viscosity estimated with the Cross equation, was compared to the temperature dependence of the time constant τ, also from the Cross model, and of the shift factor a_T used to superimpose G' and G'' (Fig. 4A–C). The Arrhenius equation fitted pretty well the experimental data, predicting a similar value for the activation energy. This parameter indicates the energy required for an elementary flow process to occur (Rao, 1999), and is dependent on polymer concentration, ionic strength, polymer physicochemical characteristics and on the shear stress applied. The activation energy was also calculated using the apparent viscosity measured for two different values of shear rate, 1 and 10 s^{-1} (Fig. 4D), and was compared to the value obtained with the zero-shear rate viscosity. As expected, the activation energy decreased as the shear rate increased (from 39.3 ± 2.4 kJ/mol with η_0, to 35.5 ± 2.4 kJ/mol with η_a at $\dot{\gamma}$ = 1 s^{-1} and 26.2 ± 3.1 kJ/mol with η_a at $\dot{\gamma}$ = 10 s^{-1}). As the shear rate becomes higher, the interactions between molecules have shorter lifetimes and less energy is needed to promote viscous flow.

3.2.4. Correlation between dynamic and steady-shear properties

The steady-shear properties were correlated with the dynamic properties using the Cox-Merz rule. The apparent viscosity, η_a, in steady shear and the complex viscosity, $|\eta^*|$, in dynamic shear, were plotted against the shear rate and the frequency, respectively. Identical results were obtained for all temperatures studied. Fig. 5 presents only the correlations obtained at 15, 35, 45 and 65 °C, for clarity reasons, and it can be perceived that the EPS sample follows the Cox-Merz rule for the conditions tested, as η_a and $|\eta^*|$ are practically coincident. This fact means that similar types of molecular rearrangements are taking place in the two flow patterns over the applied shear rate and frequency ranges, as the temperature was varied (Xu, Willför, Holmlund, & Holmbom, 2009). The EPS behaves like many polysaccharides from different sources, namely galactomannans extracted from plants (Sittikijyothin, Torres, & Gonçalves, 2004). However, other microbial polysaccharides, such as *Aeromonas* gum (Xu et al., 2006) and xanthan (Rochefort & Middleman, 1987), as well as chitosan solutions (Cho, Heuzey, Bégin, & Carreau, 2006), *Mucuna flagellipes* seed gum (Nwokocha & Williams, 2009b) and gum exudates aqueous dispersions (Rincón, Muñoz, León de Pinto, Alfaro, & Calero, 2009), did not follow the Cox-Merz rule for the conditions studied, which was attributed to aggregation/week association between polymer chains, structure decay due to the strain deformation applied to the system or to the existence of gel-like structures.

The EPS dynamic viscosity (η') is also plotted in Fig. 5, only for the temperatures of 65 and 45 °C, in order to show the results more clearly. The dynamic viscosity approached the zero-shear rate viscosity at low shear rate and frequency values for all temperatures, but it diverges gradually as the shear rate and frequency increase. In addition, the difference between η' and η_a becomes higher as the temperature decreases. This feature is common in polysaccharide

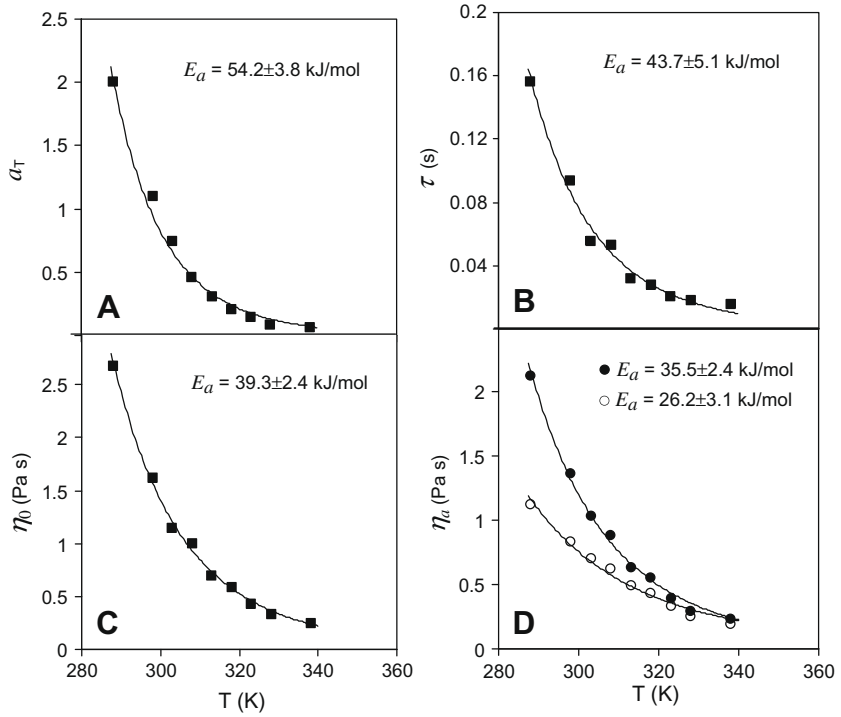

Fig. 4. Temperature dependence of: horizontal shift factor used to superimpose the dynamic moduli (A); time constant of the Cross model (B); zero-shear rate viscosity estimated by the Cross model (C); and apparent viscosity at $\dot{\gamma} = 1 s^{-1}$ (full symbols) and at $\dot{\gamma} = 10\ s^{-1}$ (open symbols) (D). The lines correspond to the fitting of the Arhenius equation.

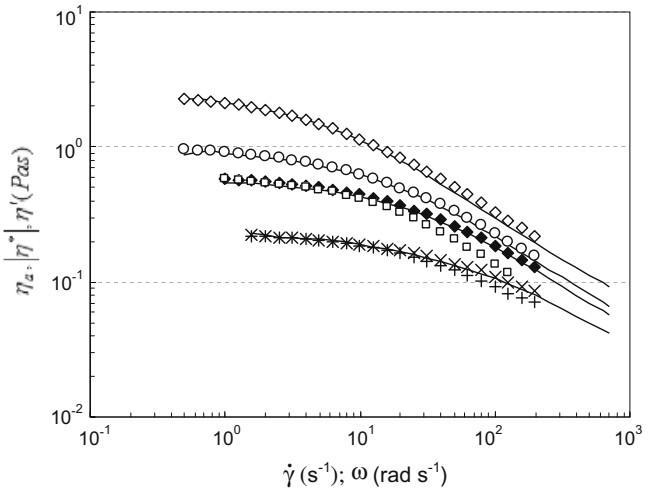

Fig. 5. Cox-Merz plot for a 0.85 wt% EPS solution at different temperatures. The apparent viscosity is represented by the solid lines; the complex viscosity by (◇) 15 °C, (○) 35 °C, (●) 45 °C and (×) 65 °C; and the dynamic viscosity by (□) 45 °C and (+) 65 °C.

solutions and may be attributed to significant differences in the molecular motions involved in dynamic and steady shears at high frequency and shear rate (Sittikijyothin et al., 2004).

The effect of successive heating and cooling stages on the dynamic and steady-shear properties of the purified EPS solution was also studied. As so, cycles of consecutive heating and cooling steps were performed with the same sample solution. After recording the mechanical spectrum and the steady-state data at 25 °C, the sample was heated up to 40 °C at a rate of 3 °C/min, followed by an oscillatory time sweep (strain = 0.2 and $\omega = 1$ Hz) at that temperature for 10 min, before cooling it down at a rate of −3 °C/min to 25 °C followed by another oscillatory time sweep (strain = 0.2 and $\omega = 1$ Hz) at that temperature for 10 min, and finally performing new dynamic and steady shear measurements. The cycle was consecutively repeated, by heating the sample up to 55, 70 and 80 °C. The flow curves and the mechanical spectra determined at 25 °C, after exposing the sample to the referred temperatures, were compared to the initial data (Fig. 6A and B). It can be observed that the flow curves and the dynamic moduli are practically coincident throughout the temperature cycles. In addition, the Cox-Merz rule continues to apply at the end of each cycle (see insert in Fig. 6B the Cox-Merz plot of the sample after being heated at 80 °C). From this, we may conclude that the EPS sample is quite stable under temperature fluctuations, maintaining its properties in consecutive oscillatory and steady-state tests at 25 °C, after being exposed to increasing temperatures up to 80 °C. These characteristics let us think that the EPS could be used in aqueous formulations (e.g. food products) that are subjected to temperature fluctuations during processing.

4. Conclusions

The EPS produced by *P. oleovorans* NRRL B-14682 using glycerol byproduct from the biodiesel production revealed to have good viscous enhancement ability and a pseudoplastic fluid behaviour. There was a total and immediate recovery of the apparent viscosity at low shear rates, after being subjected at high shear rates (up to 700 s^{-1}) for all temperatures studied. In addition, the mechanical spectra before and after the steady shear measurements were coincident, meaning that the viscoelastic properties did not change with the application of high shear stresses.

The consequence of increasing temperature was the decrease of the steady shear (η_a and η_0) and dynamic (G', G'', $|\eta^*|$ and η') parameters, due to the increase of polymer chain mobility. The Time–Temperature Superposition principle was successfully applied, especially for temperatures below 50 °C. Above that, a difference was detected on the horizontal shift factor values (a_T) used to

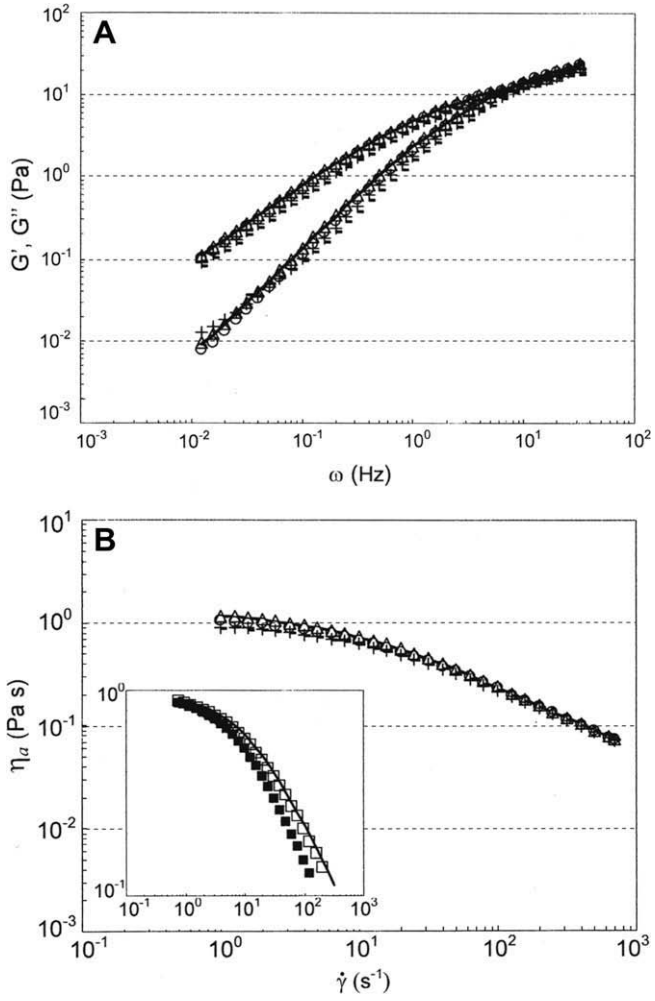

Fig. 6. Mechanical spectra (A) and flow curves (B) of a 0.85 wt% EPS sample subjected to temperature cycles. The symbols correspond to the data obtained at 25 °C after maintaining the sample during 10 min at (△) 40 °C, (○) 55 °C, (+) 70 °C and (−) 80 °C, consecutively. The solid lines represent the initial data at 25 °C. The Cox-Merz plot of the sample after being heated at 80 °C is presented in the insert: η_a (solid line), $|\eta^*|$ (open symbols) and η' (full symbols).

superimpose the curves, which may indicate a slightly different dependence on temperature of the different interactions that can occur between polymer molecules. The Arrhenius equation was used with success to describe the temperature dependence of η_0 (estimated with the Cross equation), a_T, relaxation time τ (from the Cross equation), and of the apparent viscosity at different shear rates. A decrease of the calculated activation energy was noticed with the increase of the shear rate, which is explained by a lower resistance to viscous flow. The EPS solution followed also the Cox-Merz rule, and maintained its rheological properties under consecutive oscillatory and steady-state tests at 25 °C, after being exposed to increasing temperatures up to 80 °C. We may conclude that the EPS solutions are thermorheologically simple and stable, with the same mechanisms occurring at different temperatures but at a different rate. Besides its unquestionable scientific interest, industrial applications in which temperature variations are present, at least from 15 up to 80 °C, should be considered and studied.

Acknowledgements

This project was financially supported by 73100, Lda, under the project "Production of biopolymers from glycerol", 2005/2008. Vítor D. Alves acknowledges Fundação para a Ciência e a Tecnologia, Pos-doc fellowship SFRH/BPD/26178/2005. The authors acknowledge Prof. Ana Ramos from CQFB/REQUIMTE, FCT-UNL, for the molecular weight determination.

References

Abdou, E. S., Nagy, S. S. A., & Elsabee, M. Z. (2008). Extraction and characterization of chitin and chitosan from local sources. *Bioresource Technology, 99*(5), 1359–1367.

Arvidson, S. A., Rinehart, B. T., & Gadala-Maria, F. (2006). Concentration regimes of solutions of levan polysaccharide from *Bacillus* sp. *Carbohydrate Polymers, 65*(2), 144–149.

Bae, I. Y., Oh, I., Lee, S., Yoo, S., & Lee, H. G. (2008). Rheological characterization of levan polysaccharides from *Microbacterium laevaniformans*. *International Journal of Biological Macromolecules, 42*(1), 10–13.

Carreau, P. J. (1972). Rheological equations for molecular network theories. *Transactions of the Society of Rheology, 16*, 99–127.

Cerqueira, M. A., Pinheiro, A. C., Souza, B. W. S., Lima, A. M. P., Ribeiro, C., Miranda, C., et al. (2009). Extraction, purification and characterization of galactomannans from non-traditional sources. *Carbohydrate Polymers, 75*(3), 408–414.

Cho, J., Heuzey, M., Bégin, A., & Carreau, P. J. (2006). Viscoelastic properties of chitosan solutions: Effect of concentration and ionic strength. *Journal of Food Engineering, 74*(4), 500–515. 18.

Cross, M. M. (1965). Rheology of non-Newtonian fluids: A new flow equation for pseudoplastic systems. *Journal of Colloid Science, 20*, 417–437.

Da Silva, J. A. L., Gonçalves, M. P., & Rao, M. A. (1994). Influence of temperature on the dynamic and steady-shear rheology of pectin dispersions. *Carbohydrate Polymers, 23*, 77–87.

Ferry, J. D. (1980). *Viscoelastic properties of polymers*. New york: John Willey.

Freitas, F., Alves, V. D., Pais, J., Costa, N., Oliveira, C., Mafra, L., et al. (2009a). Characterization of an extracellular polysaccharide produced by a *Pseudomonas* strain grown on glycerol. *Bioresource Technology, 100*, 859–865.

Freitas, F., Alves, V. D., Carvalheira, M., Costa, N., Oliveira, R., & Reis, M. A. M. (2009b). Emulsifying behaviour and rheological properties of the extracellular polysaccharide produced by *Pseudomonas oleovorans* grown on glycerol byproduct. *Carbohydrate Polymers, 78*(3), 549–556.

García-Ochoa, F., Santos, V. E., Casas, J. A., & Gómez, E. (2000). Xanthan gum: Production, recovery, and properties. *Biotechnology Advances, 18*, 549–579.

Gomez, C. G., Lambrecht, M. V. P., Lozano, J. E., Rinaudo, M., & Villar, M. A. (2009). Influence of the extraction–purification conditions on final properties of alginates obtained from brown algae (*Macrocystis pyrifera*). *International Journal of Biological Macromolecules, 44*(4), 365–371.

Hilliou, L., Freitas, F., Oliveira, R., Reis, M. A. M., Lespineux, D., Grandfils, C., et al. (2009). Solution properties of an exopolysaccharide from a *Pseudomonas* strain obtained using glycerol as sole carbon source. *Carbohydrate Polymers, 78*(3), 526–532.

Hilliou, L., Larotonda, F. D. S., Abreu, P., Ramos, A. M., Sereno, A. M., & Gonçalves, M. P. (2006). Effect of extraction parameters on the chemical structure and gel properties of κ/ι-hybrid carrageenans obtained from *Mastocarpus stellatus*. *Biomolecular Engineering, 23*(4), 201–208.

Nickerson, M. T., Paulson, A. T., & Speers, R. A. (2004). Time–temperature studies of gellan polysaccharide gelation in the presence of low, intermediate and high levels of co-solutes. *Food Hydrocolloids, 18*(5), 783–794.

Nwokocha, L. M., & Williams, P. A. (2009a). New starches: Physicochemical properties of sweetsop (*Annona squamosa*) and soursop (*Anonna muricata*) starches. *Carbohydrate Polymers, 78*(3), 462–468.

Nwokocha, L. M., & Williams, P. A. (2009b). Isolation and rheological characterization of *Mucuna flagellipes* seed gum. *Food Hydrocolloids, 23*(5), 1394–1397.

Peña, C., Trujillo-Roldán, M. A., & Galindo, E. (2000). Influence of dissolved oxygen tension and agitation speed on alginate production and its molecular weight in cultures of *Azotobacter vinelandii*. *Enzyme and Microbial Technology, 27*, 390–398.

Rao, M. A. (1999). *Rheology of fluids and semisolid foods: Principles and Applications*. Gaithersburg: Aspen Publishers.

Rinaudo, M. (2004). Role of substituents on the properties of some polysaccharides. *Biomacromolecules, 5*, 1155–1165.

Rincón, F., Muñoz, J., León de Pinto, G., Alfaro, M. C., & Calero, N. (2009). Rheological properties of *Cedrela odorata* gum exudate aqueous dispersions. *Food Hydrocolloids, 23*(3), 1031–1037.

Rochefort, W. E., & Middleman, S. (1987). Rheology of xanthan gum: Salt, temperature, and strain effects in oscillatory and steady shear experiments. *Journal of Rheology, 31*(4), 337–369.

Roth, L. E., Vega, D. A., Vallés, E. M., & Villar, M. A. (2004). Viscoelastic properties of networks with low concentration of pendant chains. *Polymer, 45*(17), 5923–5931.

Simsek, S., Mert, B., Campanella, O. H., & Reuhs, B. (2009). Chemical and rheological properties of bacterial succinoglycan with distinct structural characteristics. *Carbohydrate Polymers, 76*(2), 320–324.

Sittikijyothin, W., Torres, D., & Gonçalves, M. P. (2004). Modelling the rheological behaviour of galactomannan aqueous solutions. *Carbohydrate Polymers, 59*, 339–350.

Villanueva, R. D., Sousa, A. M. M., Gonçalves, M. P., Nilsson, M., & Hilliou, L. (2009) Production and properties of agar from the invasive marine alga, *Gracilaria vermiculophylla* (Gracilariales, Rhodophyta). *Journal of Applied Phycology*, doi:10.1007/s10811-009-9444-7.

Vinogradov, G. V., & Malkin, A. Ya. (1980). Rheology of polymers. Moscow: Mir Publishers.

Wang, S., Chen, F., Wu, J., Wang, Z., Liao, X., & Hu, X. (2007). Optimization of pectin extraction assisted by microwave from apple pomace using response surface methodology. *Journal of Food Engineering, 78*(2), 693–700.

Xu, X., Liu, W., & Zhang, L. (2006). Rheological behavior of Aeromonas gum in aqueous solutions. *Food Hydrocolloids, 20*, 723–729.

Xu, C., Willför, S., Holmlund, P., & Holmbom, B. (2009). Rheological properties of water-soluble spruce *O*-acetyl galactoglucomannans. *Carbohydrate Polymers, 75*, 498–504.